Photon emission from hot electrons in silicon

S. Villa, A. L. Lacaita, and A. Pacelli
Politecnico di Milano, Dipartimento di Elettronica e Informazione and Centro di Elettronica Quantistica e Strumentazione Elettronica, Consiglio Nazionale delle Ricerche, Piazza Leonardo da Vinci 32, 20133 Milano, Italy
(Received 12 December 1994; revised manuscript received 31 May 1995)

In this work we present a theoretical calculation of the photon emission spectrum via direct and phonon-assisted intra-conduction-band transitions, assessing the impact of the approximations usually made in theoretical analysis of the phenomenon. We have compared our results to a previous work, finding a marked disagreement. Our phonon-assisted emission spectrum has a much lower effective temperature, so that it overwhelms the contribution of direct processes over the range of photon energies spanning from infrared to near-UV. We discuss qualitative arguments supporting our results presenting also a simplified model suitable for a much more efficient implementation of the spectrum calculation.

I. INTRODUCTION

Light emission from hot carriers in silicon devices has been observed since the 1950s,[1] and has received much attention in recent years with the experimental analysis of photon emission from metal-oxide-semiconductor field-effect transistors (MOSFET's).[2,3] The emission of a photon due to the relaxation of a high-energy electron is called *direct* if it occurs via an electron-photon interaction only, instead it is called *indirect* if a third particle assists the process. The third particle usually supplies momentum to the electron, as the photon carries energy, but almost no momentum.

At the beginning, two mechanisms were proposed to explain this phenomenon: bremsstrahlung processes, where the momentum is supplied by a charged center, and a recombination between electrons and holes. These conclusions were drawn on the basis of semiclassical models.[4] However, recent experimental evidences have ruled out any contribution from impurity-assisted processes[5] and electron-hole recombination.[6] Furthermore, Bude *et al.*[7] have recently performed a theoretical calculation for direct (D), phonon-assisted (PA), and impurity-assisted (IA) transition rates in silicon devices. Their results show that for a typical n-MOSFET, the contribution of recombination and IA processes is negligible (except for impurity densities higher than $5\times10^{20}\,\mathrm{cm}^{-3}$), while most of the photons with energy below 2 eV are emitted from direct processes. Above 2 eV PA, processes become dominant.

In this work, we critically review the calculations of the photon emission from hot electrons. First, we present our refinements to the computational model of Ref. 7, namely: (i) The introduction of a finite lifetime of the initial state in second-order transitions, and (ii) the use of a more realistic photon density of states.

Then we show that our calculated PA spectrum is markedly different from that of Ref. 7 leading to a dominant contribution over all the considered spectral range. Finally, we comment on these results presenting a simplified model that presents much less computational requirements nevertheless leading to results in very good agreement with those previously obtained from the more detailed calculations.

II. THEORETICAL FRAMEWORK

A. Direct processes

Direct transition rates have been calculated from a first-order perturbation theory, using the Fermi golden rule. The probability per unit time of a radiative transition from an initial Bloch state $|\nu,\mathbf{k}\rangle$ to the final state $|\nu',\mathbf{k}'\rangle$ is given by

$$W=\frac{2\pi}{\hbar}\left|\langle\nu',\mathbf{k}'|H_\omega|\nu,\mathbf{k}\rangle\right|^2\delta(E-E'-\hbar\omega), \tag{1}$$

where E and E' are the energies of the initial and final electron states, and H_ω is the electron-photon interaction Hamiltonian. Since in the frequency range of interest the photon modes have negligible occupation, in the following, we will only consider spontaneous emission processes; the interaction Hamiltonian for the emission a photon of momentum $\mathbf{q}$ and polarization λ is

$$H_\omega=\frac{-e}{m_0}\sqrt{\frac{\hbar}{2\epsilon(\omega,0)\omega\Omega}}e^{i\mathbf{q}\cdot\mathbf{r}}i\hbar\mathbf{e}_\lambda\cdot\vec{\nabla}, \tag{2}$$

where e is the electron charge; m_0 is the electron rest mass; $\epsilon(\omega,0)$ the long-wavelength, energy-dependent dielectric function; $\mathbf{e}_\lambda$ the unit polarization vector; $\hbar\omega$ the photon energy; and Ω is the volume of the crystal.

The evaluation of the matrix element leads to the momentum conservation rule $\mathbf{k}'=\mathbf{k}+\mathbf{q}+\mathbf{G}$. Since q is very small in normal processes ($\mathbf{G}=0$), the states $|\nu,\mathbf{k}\rangle$ and $|\nu',\mathbf{k}'\rangle$ have almost the same wave vector ($\mathbf{k}\approx\mathbf{k}'$) and the number of umklapp processes ($\mathbf{G}\neq0$) is negligible because they occur only at the very borders of the Brillouin zone. By neglecting the polarization of the

emitted light, the rate given by Eq. (1) must be averaged over all the possible orientations of $\mathbf{e}_\lambda$.[9] This procedure is equivalent to replace the dot product in Eq. (2) with its average on the solid angle, that is

$$\mathbf{e}_\lambda \cdot \vec{\nabla} \rightarrow \sqrt{\frac{1}{3}}\nabla. \tag{3}$$

The monochromatic emission rate $1/\tau_{\rm em}(\hbar\omega)$ for a given initial state $|\nu, \mathbf{k}\rangle$ is obtained by integrating the obtained single-transition rate over final states. Formally, at this stage, we should take into account the probability for the final state to be already occupied, however, this occurrence can be neglected because we are not dealing with a degenerate semiconductor.

The resulting expression is

$$\frac{1}{\tau_{\rm em}(\omega)} = \frac{2\pi}{\hbar}\sum_{\nu'}\frac{e^2}{m_0^2}\left(\frac{\hbar}{2\omega\,\epsilon(\omega,0)}\right) \times \frac{1}{3}\left|\hbar\langle\nu', \mathbf{k}|\nabla|\nu, \mathbf{k}\rangle\right|^2 \rho(\hbar\omega)d\omega, \tag{4}$$

where $\rho(\hbar\omega)$ is the photon density of states.

Note that the integration over the final states has been split into a sum over the band index ν' and an integration over photon modes. Since the photon momentum is small, it can be assumed that the matrix elements do not depend on $\mathbf{q}$ and this latter integration reduces to a multiplication of the rate given by Eq. (1) by the number of photon states with frequency between ω and $\omega + d\omega$ given by

$$\rho(\hbar\omega)d(\hbar\omega) = \frac{\Omega\omega^2 n^3}{\hbar\pi^2 c_0^3}\left|1 + \frac{\omega}{n}\frac{dn}{d\omega}\right| d(\hbar\omega), \tag{5}$$

where $n = \sqrt{\epsilon(\omega, 0)}$ is the refractive index. The frequency dependence of the dielectric function $\epsilon(\omega)$ was neglected in Ref. 7. Although the variation of the refractive index with energy is not dramatic, its derivative with respect to energy strongly affects the photon density of states [cfr. Eq. (5)], which is directly proportional to the emission rate. In fact, as the refractive index of silicon varies from about 3.5 at low frequencies to about 7 at 3 eV, the photon density of states is enhanced by one order of magnitude at 3 eV (Fig. 1). Although this effect is attenuated by the presence of the factor $\epsilon(\omega, 0)$ in the denominator of Eq. (4), there is still an enhancement of the spectrum by a factor of 4 at 3 eV. Therefore, we have used the experimental energy-dependent refractive index[10] in Eq. (4) and in all subsequent calculations.

The rate of emitted photons per unit time and energy has been finally obtained by integrating Eq. (4) over the initial states.

$$W(\hbar\omega) = \frac{\Omega}{8\pi^3}\int\sum_{\nu} f(\nu, \mathbf{k})\frac{1}{\tau_{\rm em}(\omega)}\mathbf{d}^3\mathbf{k}, \tag{6}$$

where $f(\nu, \mathbf{k})$ is the occupation probability of the electron state $|\nu, \mathbf{k}\rangle$. In our calculations, we have chosen the normalization factor for $f(\nu, \mathbf{k})$, satisfying the condition

$$2\frac{\Omega}{8\pi^3}\int\sum_{\nu} f(\nu, \mathbf{k})\mathbf{d}^3\mathbf{k} = 1, \tag{7}$$

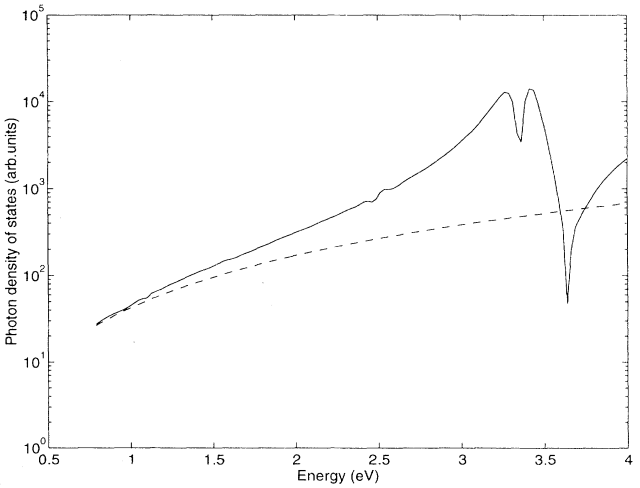

FIG. 1. Photon density of states, as calculated from the energy-dependent dielectric function (solid line) and for a constant refractive index (dashed line).

which corresponds to the presence of one electron in the crystal volume.

B. Phonon-assisted processes

The computation of PA radiative scattering rates has been done using second-order perturbation theory; the expression of the probability per unit time of a given PA transition is

$$W = \frac{2\pi}{\hbar}|M_{12}|^2\,\delta(E - E' - \hbar\omega \pm \hbar\omega_0), \tag{8}$$

where the sign $\pm$ corresponds to absorption or emission of a phonon with energy $\hbar\omega_0$. This expression is quite similar to Eq. (1), but in this case, the matrix element M_{12} has a more complicated form. For the sake of simplicity, in the following, we will label the eigenstates of the overall system with a unique index comprehensive of both the quantum numbers of the electron and the fields; the initial state is $|i\rangle$ and the final state $|f\rangle$. Moreover, we will give the analytical expressions only for a transition with both phonon and photon emissions. In this case, the second-order matrix element is

$$M_{12} = \sum_v \frac{\langle f|H_\omega + H_0|v\rangle\langle v|H_\omega + H_0|i\rangle}{E_v - E_i}, \tag{9}$$

where the sum over $|v\rangle$ is performed over all the possible intermediate (or *virtual*) states. The energies E_i, E_v are now the total energies of the system electron+fields in the initial and the intermediate state, respectively. The selection rules for the virtual states are imposed by momentum and spin conservation, but not by energy conservation. In fact, a transition can violate energy conservation of a quantity $\Delta E = E_v - E_i$ provided that its characteristic time scale is shorter than $\hbar/\Delta E$. This

condition is the physical origin of the denominators in Eq. (9), where the matrix elements are proportional to the transition lifetimes for the virtual state $|v\rangle$,

$$\tau_v \simeq \frac{\hbar}{|E_v - E_i|}. \tag{10}$$

The constraints imposed by momentum conservation reduce the virtual states to the Bloch eigenstates, with one of two possible wave vectors, namely, $\mathbf{k}'_v = \mathbf{k}_i - \mathbf{q}$ *or* $\mathbf{k}''_v = \mathbf{k}_i - \mathbf{q_0}$, where $\mathbf{k}_i$ and $\mathbf{k}_v$ are the wave vectors of the electron in the initial and intermediate state, $\hbar\mathbf{q}$ the momentum of the emitted photon, and $\hbar\mathbf{q_0}$ the momentum of the emitted phonon. The states with the first wave vector $\mathbf{k}'_v$ arise as intermediate states in processes, where the interaction with the photon precedes that with the phonon; in the following, these processes will be called type (A). On the other hand, states with the wave vectors $\mathbf{k}''_v$ occur as virtual states on the processes, where the interaction order is reversed: They will be called type (B) processes.

Separating the contributions of (A) and (B) processes, the matrix element can be written as

$$\begin{aligned} M_{12} &= M_{12}^{v'} + M_{12}^{v''} \\ &= \sum_{v'} \frac{\langle f|H_0|v'\rangle\langle v'|H_\omega|i\rangle}{E_{v'} - E_i} \\ &\quad + \sum_{v''} \frac{\langle f|H_\omega|v''\rangle\langle v''|H_0|i\rangle}{E_{v''} - E_f}. \end{aligned} \tag{11}$$

The matrix elements of the interaction Hamiltonians are null if the intermediate Bloch state is already occupied. Therefore, excluding the case of a degenerate n-doped semiconductor, we can sum over conduction band states only.

As regards the analytical form of the second-order matrix elements, it must be noted that they have real poles which, from a numerical standpoint, could cause instabilities on the integration algorithm. However, this poses no problems because, in the cases where the denominators vanish, some approximations assumed in the derivation of Eq. (8) break down; the most important one is that state decay is neglected. In fact, a more rigorous approach should take into account the finite lifetime of electron states leading to equations similar to (7) and (8), in which an electron self-energy appears in the denominators, shifting the poles into the complex plane. In addition the Dirac δ function should be replaced by a spectral energy function. However, this latter refinement would result only in a slight smoothing of the emission spectra at the cost of a great increase of the computational requirements and it has been neglected. The self-energy introduction brings instead significative changes in the results, because the imaginary part of the self-energy Γ takes into account the damping of quasiresonant transitions. In these cases, the standard second-order perturbation theory would predict transition lifetimes unphysically longer than the lifetimes of the Bloch states involved. Therefore, we have used transition matrix elements in the form:

$$\begin{aligned} M_{12} &= \sum_{v'} \frac{\langle f|H_0|v'\rangle\langle v'|H_\omega|i\rangle}{E_{v'} + \hbar\omega - E_i + i\Gamma_i} \\ &\quad + \sum_{v''} \frac{\langle f|H_\omega|v''\rangle\langle v''|H_0|i\rangle}{E_{v''} + \hbar\omega_0 - E_i + i\Gamma_i}. \end{aligned} \tag{12}$$

In this equation, we have explicitly divided the total energy of the intermediate state into electron energy (E_v) and emitted particle energy ($\hbar\omega$ or $\hbar\omega_0$). It should be noted that the introduction of Γ_i does not affect matrix elements of nonresonant transitions, since the real part of the denominators in Eq. (12) is dominant.

We have estimated the self-energy using the Born approximation and retained only the imaginary part Γ_i, since the real part is of the order of few tens of meV and is, therefore, negligible. Γ_i is given by

$$\Gamma_i = \frac{\hbar}{2\tau_i}, \tag{13}$$

where $1/\tau_i$ is the scattering rate for the initial state taken from the energy-dependent scattering rate obtained from full-band Monte Carlo simulations.[11] In order to refine the calculation, either the Fock approximation for the self-energy insertion or the finite lifetime of the intermediate state could be introduced in the calculation; however, this would only give higher-order corrections, with respect to the framework of present calculations; therefore, we have not included these refinements in the computational model.

The nonpolar electron-phonon Hamiltonian for an electron in the state $|\nu, \mathbf{k}\rangle$ and an emitted phonon of the ηth branch is given by

$$H_0 = \sqrt{\frac{\hbar(n_{\eta,\mathbf{q_0}} + 1)}{2\rho\Omega\omega_{\eta,\mathbf{q_0}}}}\Delta_\eta(\mathbf{k}, \mathbf{k}', \nu, \nu')e^{i\mathbf{q_0}\cdot\mathbf{r}}, \tag{14}$$

where ρ is the mass density of silicon and $n_{\eta,\mathbf{q}}$ is the phonon occupation number given by a Bose-Einstein distribution at the lattice temperature. The quantity $\Delta_\eta(\mathbf{k}, \mathbf{k}', \nu, \nu')$ is often referred to as deformation potential. It could be obtained from pseudopotential calculations, at least for small wave vectors.

The transition probability of Eq. (12) must be integrated over initial and final Bloch states, over the photon mode and the phonon mode. The integration over the four wave vectors can be reduced to an integration over $\mathbf{k}$ and $\mathbf{k}'$. This is done by using momentum conservation to eliminate the integration over phonon momentum and then supposing that, as in the direct case, transitions differing only by the wave vector of the emitted photon have nearly the same probability and so replacing the integration over $\mathbf{q}$ with a simple multiplication by the optical density of states (5). The resulting emission rate per unit time and energy is then

$$\begin{aligned} S(\hbar\omega) = \frac{\Omega^2}{(2\pi)^6} \int\int \sum_{\nu_i} \sum_{\nu_f} \frac{2\pi}{\hbar} \rho(\hbar\omega) d(\hbar\omega) \, |M_{12}|^2 \\ \times \delta(E - E' - \hbar\omega \pm \hbar\omega_0) f(\mathbf{k}_i, \nu_i) \mathbf{d}^3\mathbf{k}_i \, \mathbf{d}^3\mathbf{k}_f. \end{aligned} \tag{15}$$

III. NUMERICAL IMPLEMENTATION

The calculation of the emission spectra from direct transitions requires the three-dimensional integration of Eq. (4) over initial states in $\mathbf{k}$ space, weighted by the electron distribution. We have used a histogram method with a uniform integration mesh fine enough to properly manage the dependence of the electron-photon matrix element on wave vector. More precisely, we adopted a grid with 88 points on the $\Gamma - X$ axis and 60951 points in the irreducible wedge (IW). This calculation poses no relevant numerical problems or CPU requirements.

The calculation of the PA light emission is much more time consuming, because it requires a six-dimensional integration over the Brillouin zone. Moreover, the second-order matrix element $M_{12}(\mathbf{k},\mathbf{k}')$ strongly depends on the wave vectors $\mathbf{k}$ and $\mathbf{k}'$, due to changes of both the virtual-state lifetimes and the photon matrix elements. Therefore, some simplifications are needed to numerically handle the calculation. Regarding the electron-phonon interaction, we have chosen the model implemented in the device analysis using Monte Carlo and Poisson solver (DAMOCLES) full-band Monte Carlo.[12] In this model, the approximated phonon dispersion is composed by three distinct branches only: longitudinal acoustic, transversal acoustic, and optical; the matrix elements are in the same form as in Eq. (14), where the deformation potentials are taken as the product of an isotropic coupling constant $\Delta_\eta(q_0,\nu,\nu')$ and an analytic overlap factor,

$$I(\mathbf{k},\mathbf{k}') = 3\frac{x\cos(x) - \mathrm{sen}(x)}{x^3} \quad ; \quad x = |\mathbf{k}' - \mathbf{k}|R_0, \quad (16)$$

where the constant R_0 is taken equal to the radius of a sphere with half the volume of the primitive lattice cell.[13]

The dependence of $\Delta_\eta(q_0,\nu,\nu')$ on phonon wave vector module $\mathbf{q_0}$ is taken as linear for the two acoustic modes, and constant for the optical one. Following the notation of Ref. 12, the deformation potentials are given by $\Delta_{\mathrm{LA}}q_0$ for longitudinal-acoustic phonons, $\Delta_{\mathrm{TA}}q_0$ for transverse acoustic, and to DK_{OP} for optical ones. In Ref. 12, two sets of coupling constants are reported; the first, labeled as "first band," has to be used for phonon scattering between two electronic states both belonging to the first conduction band; otherwise, the values of the set labeled "other bands" must be used. This model can estimate only the magnitude of the electron-phonon matrix elements without giving information about its phase. This does not affect the calculation of first-order processes, but for higher order processes there is quantum interference between indistiguishable transitions; therefore, the knowledge of the phases of all the matrix elements is, in principle, required. However, we will show in the following that the absence of significant correlations makes quantum interference negligible in the calculation.

It must be noted that the $\mathbf{k}$ dependence of our electron-phonon matrix element is due to that of the overlap factor only, which is a slowly varying function compared to both transition lifetimes and electron-photon matrix element.

We have exploited this property by using two different meshes in $\mathbf{k}$ space: a fine grid for the computation of the electron-photon interactions and the bands eigenvalues; a very coarse grid (89 points in the IW) for the overlap integrals. Band eigenvalues and matrix elements were calculated with a three-parameter local empirical pseudopotential method;[8] more precisely only the lowest four conduction bands were considered and a plane wave basis of 137 G vectors in the reciprocal space was used. Care was taken in order to avoid sampling the coarse mesh on symmetry points, where numerical problems can occur, due to degeneracy. The PA emission was obtained using Eq. (15), neglecting light polarization and quantum interference. This means that we have integrated transitions rates, in which the squared magnitude of matrix elements $|M_{12}|^2$ has been replaced by

$$\sum_{v'}\left|\frac{\langle f|H_0|v'\rangle\langle v'|H_\omega|i\rangle}{E_{v'}+\hbar\omega-E_i+i\Gamma_i}\right|^2 + \sum_{v''}\left|\frac{\langle f|H_\omega|v''\rangle\langle v''|H_0|i\rangle}{E_{v''}+\hbar\omega_0-E_i+i\Gamma_i}\right|^2, \quad (17)$$

where the operator H_ω is the scalar operator that can be obtained by performing the substitution (3) in the operator given by Eq. (2). The scalar properties of the obtained electron-photon Hamiltonian joined with the particular isotropic form of the electron-phonon Hamiltonian can be used to fully exploit crystal symmetries, thus reducing both initial and final-state wave vector integration into the irreducible wedge.

IV. RESULTS

The direct and PA spectra have been calculated for a sample electron energy distribution (EED) also considered in Ref. 7. The EED is a Gaussian fit of a Monte Carlo simulation for an n-MOSFET.[14] Figure 2 shows

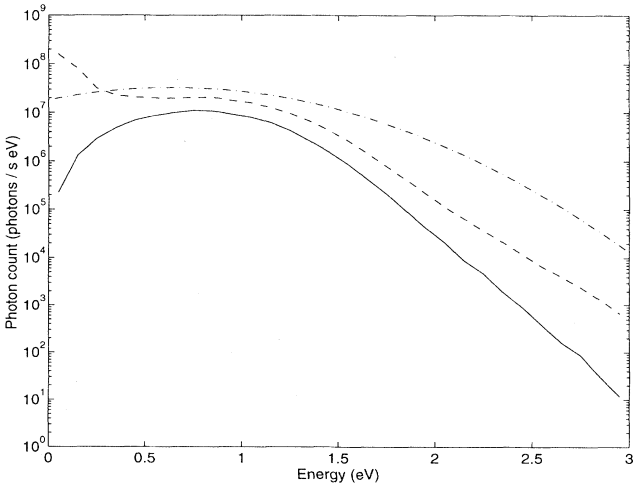

FIG. 2. Comparison between direct (solid line) and PA spectra (dashed line) for a sample electron distribution, shown in arbitrary units (dashed-dotted line).

the calculated spectra (in photons/s eV) along with the EED (in arbitrary units).

It is interesting to assess the role of the initial-state lifetime on the calculation of the PA spectrum. From a numerical standpoint, the $i\Gamma_i$ term in Eq. (12) limits the magnitude of the terms when the energy differences $E_{v'} - E_i + \hbar\omega \pm \hbar\omega_0$ or $E_{v''} - E_f - \hbar\omega \pm \hbar\omega_0$ vanish, and the virtual-state lifetime becomes infinite causing numerical instabilities. In Ref. 7, this effect was accounted for by taking out of the sum the terms corresponding to those transitions with a virtual-state lifetime greater than the initial-state lifetime. In this way, nearly resonant transitions are overestimated (by taking $\Gamma_i = 0$), while resonant transitions are neglected. Our calculation does not need to take care of resonant transitions as a special case, as they do not make the algorithm unstable.

Figure 3 shows the effect of the initial-state lifetime on the PA spectrum. The figure compares the actual calculation for the emission rate (solid line) with the two spectra obtained by enhancing the initial-state lifetime by a factor of 200 (dashed line), and by omitting the resonant terms (dashed-dotted line) as in Ref. 7. Note that the intensity of the long-lifetime spectrum is the highest and shows a much larger numerical noise, since some terms of Eq. (12) can assume very large values at resonances in $\mathbf{k}$ space. Instead, the other two spectra are almost identical. This means that the approximations introduced by neglecting the resonant terms and the damping due to the initial state lifetime compensate each other and that, aside from physical considerations, the two models are almost equivalent.

In order to have a quantitative feeling on the impact of the quantum interference on the computed emission rate, we have fully computed the emission spectra using a slightly modified model that accounts for interference. More precisely, the squared magnitude of transition matrix elements used in this model was given by

$$\left|\sum_{v'} \frac{\langle f|H_0|v'\rangle\langle v'|H_\omega|i\rangle}{E_{v'} + \hbar\omega - E_i + i\Gamma_i}\right|^2 + \left|\sum_{v''} \frac{\langle f|H_\omega|v''\rangle\langle v''|H_0|i\rangle}{E_{v''} + \hbar\omega_0 - E_i + i\Gamma_i}\right|^2 . \quad (18)$$

In this way, we accounted for quantum interference only among processes of the same type (A or B). In this equation, the vector character of electron-photon Hamiltonian has to be taken into account explicitly summing transition rates over different polarizations; in fact, the use of the replacement (3) in interference terms should cause a loss of the phase of the electron-photon matrix element. Moreover, since we cannot make a guess about the phase of the electron-phonon matrix element it was supposed to be a positive real number. It can be easily verified that these assumptions together with the previously discussed different modeling of resonant processes lead to Eqs. (5) and (6) in Ref. 7.

The quantitative comparison between spectra obtained with or without accounting for interference has shown differences smaller than 1%. This means that the phases of the matrix elements for the various processes are almost randomly distributed; although the phase of the electron-phonon matrix element cannot be known, we can reasonably think that this would not affect the results. In fact, only a very strong correlation of this phase with respect to that of electron-photon matrix elements and energy denominators would bring interference effects to relevance. Since Ref. 7 reported only the relative comparison between direct and indirect processes and not the absolute intensity in photons per unit carrier, time, and energy, we have multiplied that results by a renormalization constant in order to equalize the two direct spectra. Figure 4 shows the comparison of our results with those

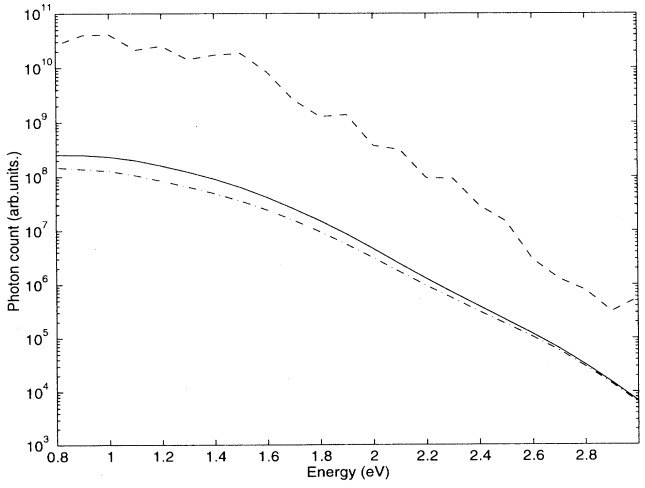

FIG. 3. PA photon spectra computed assuming a realistic initial-state lifetime (solid line), compared with the result obtained by enhancing the lifetime by a factor of 200 (dashed line) and by omitting the resonant processes as in Ref. 7 (dashed-dotted line).

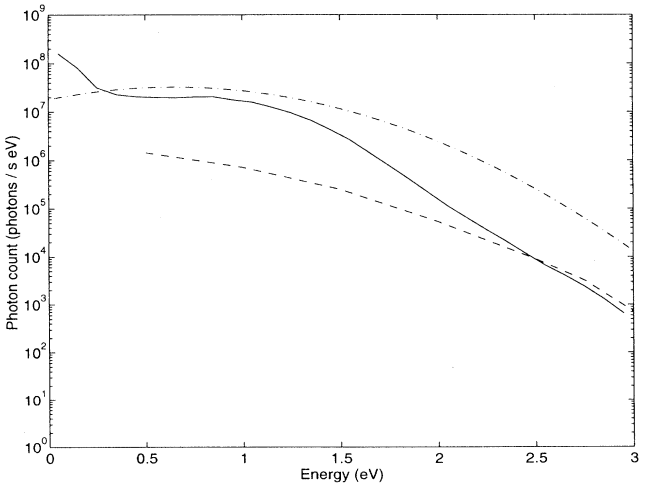

FIG. 4. Comparison between the calculated phonon-assisted (PA) spectra from this work (solid line), from Ref. 7 (dashed line), and the electron distribution in arbitrary units (dashed-dotted line).

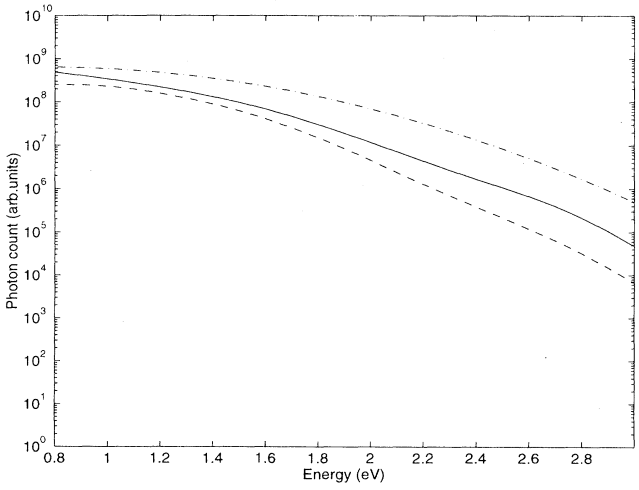

FIG. 5. Plots of the electron distribution function (dashed-dotted line) and the quantities $I(\hbar\omega)$ given by Eq. (20) (dashed line), $N(\hbar\omega)$ given by Eq. (19) (solid line).

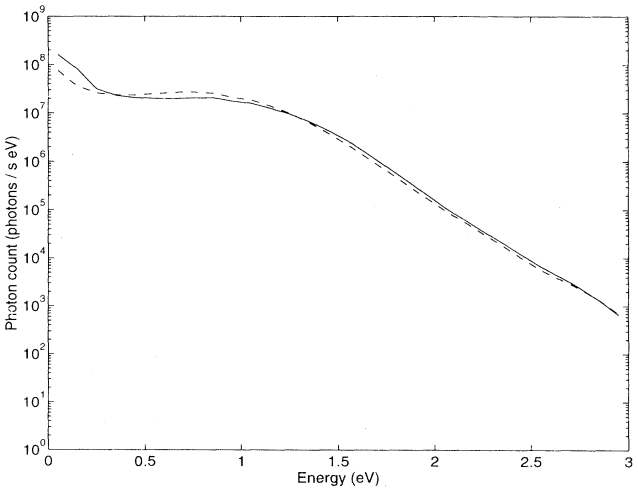

FIG. 6. Comparison between the spectrum obtained from the full calculation (solid line) and the simplified one (dashed line).

computed by Bude *et al.*[7] for the same EED. The shapes of the direct-transition spectra are identical, while the PA spectra are markedly different. More precisely, our spectrum has a lower effective temperature than the EED for energies greater than 1 eV, while the PA spectrum of Ref. 7 has a temperature higher than the EED over the entire energy range.

The frequency dependence of the dielectric function that we have used in the calculations gives an *upward* correction of the spectrum; this means that if the actual photon density of states were considered in Ref. 7, the temperature of their PA spectrum would have been even higher.

In order to check our results, we have investigated how the PA spectrum is affected by the total number of allowed transitions and by the average lifetime of the virtual states. Figure 5 shows the EED (dash-dotted line) and the dependence (solid line) of the quantity,

$$N(\hbar\omega) = \int_{\hbar\omega}^{\infty} f(E)g(E)g(E-\hbar\omega)dE, \qquad (19)$$

on the photon energy $\hbar\omega$, where $g(E)$ is the electron density of states. $N(\hbar\omega)$ gives the total number of allowed transitions, weighted by the EED, and is slightly cooler than the EED. Figure 5 also shows the dependence (dashed line) of the quantity

$$I(\hbar\omega) = \int_{\hbar\omega}^{\infty} f(E)g(E)g(E-\hbar\omega)\tau^2(E,\hbar\omega)dE, \qquad (20)$$

where $\tau(E,\hbar\omega)$ is the average lifetime of the virtual states involved in the PA transitions starting from states at energy E, with the emission of a photon $\hbar\omega$. From a physical standpoint, this corresponds to take constant both the photon and the phonon matrix elements in the numerators of Eq. (12): Note that the introduction of the virtual-state lifetime has further cooled the spectrum. Moreover, the shape of $I(\hbar\omega)$ is almost coincident with the shape of the PA spectrum previously shown in Fig. 4. This means that there is no significant correlation between the intensity of a PA transition and the energy of the emitted photon, thus making reasonable that the detailed calculation should give a spectrum cooler than the EED.

Finally, it is worth introducing a simplified model: In the assumption that the EED depends only on the electron energy, the PA emission rate given by Eqs. (15,17) can be written in the equivalent form:

$$S(\hbar\omega) = \frac{\Omega}{(2\pi)^3}\int \sum_{\nu_i}\sum_{v'} \rho(\hbar\omega)d(\hbar\omega)\left|\frac{\langle v'|H_\omega|i\rangle}{E_i - E_{v'} - \hbar\omega + i\Gamma_i}\right|^2 \tau^{-1}(\mathbf{k}_i, v', E_i - \hbar\omega)f(E_i)\mathbf{d}^3\mathbf{k}_i$$
$$+\frac{\Omega}{(2\pi)^3}\int \sum_{\nu_f}\sum_{v''} \rho(\hbar\omega)d(\hbar\omega)\left|\frac{\langle f|H_\omega|v''\rangle}{E_{v''} - E_f - \hbar\omega + i\Gamma_i}\right|^2 \tau^{-1}(\mathbf{k}_f, v'', E_f + \hbar\omega)f(E_f + \hbar\omega)\mathbf{d}^3\mathbf{k}_f, \qquad (21)$$

where we have defined

$$\tau^{-1}(\mathbf{k},\nu,E) = \frac{2\pi}{\hbar}\frac{\Omega}{(2\pi)^3}\int \sum_{\nu'} |\langle \mathbf{k},\nu|H_0|\mathbf{k}',\nu'\rangle|^2 \times\delta(E - E_{\mathbf{k}'} \pm \hbar\omega_0)\mathbf{d}^3\mathbf{k}'. \qquad (22)$$

Note that if the energy of the eigenstate $|\mathbf{k},\nu\rangle$ is equal to E, then $\tau^{-1}(\mathbf{k},\nu,E)$ is the electron-phonon scattering rate for the eigenstate. Since the final spectrum is obtained from a weighted average of many uncorrelated contributions, it is expected that the replacement

of $\tau(\mathbf{k}, \nu, E)^{-1}$ with the energy-dependent scattering rate $\tau(E)$ should lead to numerical results fairly close to those from the detailed calculations. The validity of this *ansatz* is confirmed by the comparison shown in Fig. 6.

This simplified approach leads to three major improvements:

(i) The numerical implementation of the simplified model is much more efficient, since the computational requirements have been lowered to the same order of direct transitions case.

(ii) The computation of the electron-phonon matrix elements is no longer needed; the only quantity required is the energy-dependent scattering rate, which could be found in almost any Monte Carlo published report.

(iii) In cases of extremely high-doped semiconductors, the contribution of brehmsstrahlung radiation could be easily computed by simply replacing the electron-phonon scattering rate by ionized-impurity scattering rate.

V. CONCLUSIONS

In this work, we have reported and commented upon a theoretical calculation of photon emission by direct and phonon-assisted transitions. Our analysis differs from previous work[7] in a more detailed treatment of purely quantum effects. In contrast with previous estimates, we have found that PA transitions play a key role over all the considered energy range.

ACKNOWLEDGMENTS

This work was supported by the Italian Ministry of Scientific Research and Technology and the National Research Council; we also gratefully acknowledge M. V. Fischetti and P. Vogl for helpful discussions and suggestions.

[1] A. G. Chynoweth and K. G. McKay, Phys. Rev. **102**, 369 (1956).
[2] A. Toriumi *et al.*, IEEE Trans. Electron Devices **34**, 1501 (1987).
[3] M. Lanzoni *et al.*, IEEE Electron Device Lett. **12**, 341 (1991).
[4] T. Figielsky and A. Torun, in *Proceedings of the International Conference on Physics of Semiconductors, Exeter, UK*, edited by A. Stickland (Institute of Physics, London, 1962), p. 853.
[5] H. S. Wong, IEEE Electron Device Lett. **13**, 389 (1992).
[6] A. Lacaita, F. Zappa, S. Bigliardi, and M. Manfredi, IEEE Trans. Electron Devices **40**, 577 (1993).
[7] J. Bude, N. Sano, and A. Yoshii, Phys. Rev. B **45**, 5848 (1992).
[8] M. L. Cohen and T. K. Bergstresser, Phys. Rev. **141**, 789 (1966).
[9] L. Carbone *et al.*, Semicond. Sci. Technol., **9**, 674 (1994).
[10] *Properties of Silicon*, EMIS Data Reviews Series (The Institution of Electrical Engineers, London, 1988).
[11] M. V. Fischetti, IEEE Trans. Electron Devices **38**, 634 (1991).
[12] M. V. Fischetti and J. M. Higman, in *Monte Carlo Device Simulation: Full Band and Beyond*, edited by K. Hess (Kluwer, Dordrecht, 1991).
[13] M. V. Fischetti (private communication).
[14] J. M. Higman, K. Hess, C. G. Hwang, and R. W. Dutton, IEEE Trans. Electron Devices **36**, 930 (1989).